Semiclassical trace formulas for two identical particles

Jamal Sakhr and Niall D. Whelan
Department of Physics and Astronomy, McMaster University, Hamilton, Ontario, Canada L8S 4M1
(Received 24 January 2000; published 19 September 2000)

Semiclassical periodic orbit theory is used in many branches of physics. However, most applications of the theory have been to systems that involve only single-particle dynamics. In this paper, we develop a semiclassical formalism to describe the density-of-states for two noninteracting particles. This includes accounting properly for particle exchange symmetry. As specific examples, we study two identical particles in a disk and in a cardioid. In each case, we demonstrate that the semiclassical formalism correctly reproduces the quantum densities.

PACS number(s): 03.65.Sq, 73.40.Gk, 05.45.Mt, 05.45.−a

I. INTRODUCTION

Semiclassical physics has experienced a resurgence of interest, largely due to the work of Gutzwiller [1], Balian and Bloch [2], and Berry and Tabor [3]. (For recent reviews see Refs. [4,5].) These works showed that if we separate the density-of-states into smooth and oscillatory components, then the oscillatory part is related to the dynamics of the underlying classical system via periodic orbits. This complements the earlier work of Weyl, Wigner, Kirkwood and others who showed that the smooth component is related to the geometry of the classical phase space. Actually, the two components are related in a subtle way [6,7] since the complete geometry imparts the full dynamics and vice versa.

Most of the theoretical work has concentrated on the single-particle density-of-states, however, there are some notable exceptions [8–10]. In Ref. [8], the focus is on the average level density and its extension to systems of identical particles. Specifically, the authors consider a system of N fermions in one dimension. Their Weyl formula for fermions works well for attractive two-body interactions, but overestimates the quantum staircase function when there are repulsive two-body interactions. The author of Ref. [9] develops a generalization of the canonical periodic orbit sum for the special case of N interacting spinless fermions in one dimension. It is assumed the periodic orbits are isolated and therefore it is most applicable to fully chaotic systems. The author also considers a system of noninteracting fermions and writes the many-body level density as a convolution integral involving one body level densities. Finally, we mention Ref. [10], which presents an expansion of the periodic orbit sum in terms of the particle number using ideas from Refs. [8] and [9].

Similarly, most of the applications of semiclassical theory have been to systems that involve only single-particle dynamics. Here, we mention some exceptions. The authors of Ref. [11] extend the study of scars [12] to classically chaotic few body systems of identical particles. A study of the eigenfunctions of an interacting two-particle system can be found in Ref. [13]. The semiclassical approach to the helium atom, which can be understood as two interacting electrons in the presence of a helium nucleus, has been studied in Ref. [14]. We also mention the applications of semiclassical theory to mesoscopic physics [15]. For example, orbital magnetism has been studied semiclassically for diffusive systems in Ref. [16] and for ballistic systems in Refs. [17] and [18]. For reviews, see Ref. [19].

Ultimately, one would like to study systems with an arbitrary number of interacting particles. In the present paper, we begin by exploring the structure of the trace formula for two noninteracting particles including an examination of the decomposition into bosonic and fermionic spaces. This sets the stage for the interacting N-body problem to be explored in a future publication [20]. The method employed here uses the fact that the two-particle density-of-states is the autoconvolution of the single-particle density-of-states. Subsequently, we decompose the semiclassical two-particle density-of-states into three distinct contributions and of particular interest is the contribution that contains two-particle dynamics.

Billiards have served as prominent model systems in quantum chaos. They combine conceptual simplicity (the model of a free particle in a box) while allowing the full range of classical dynamics, from integrable to chaotic. Therefore, as illustrations of the formalism, we consider quantum billiards that contain two particles. As specific examples, we study two noninteracting identical particles in a disk and in a cardioid. The former problem is integrable while the second is chaotic so these two examples provide a direct test of the formalism in the two limiting cases of classical motion.

II. BACKGROUND THEORY

A. Single-particle semiclassical theory

In this section, we review the formalism for the semiclassical decomposition of the single-particle density-of-states. Let $\{\epsilon_i\}$ be the single-particle energies so that the single-particle density-of-states is

$$\rho_1(\epsilon)=\sum_i \delta(\epsilon-\epsilon_i), \tag{1}$$

where the subscript 1 indicates that it is a single-particle density. A fundamental property of the quantum density-of-

states is that it can be exactly decomposed into an average smooth part and an oscillatory part [2]:

$$\rho_1(\epsilon)=\overline{\rho}_1(\epsilon)+\widetilde{\rho}_1(\epsilon). \tag{2}$$

There are various approaches for calculating these quantities [5]. For example, in systems with analytic potentials, the smooth part may be obtained from an extended Thomas-Fermi calculation which is an asymptotic expansion in powers of $\hbar$. In billiard systems, where the particle is confined to a spatial domain by the presence of infinitely steep potential walls, the smooth part may be obtained from the Weyl expansion. In two-dimensional billiards with piecewise smooth boundaries and Dirichlet boundary conditions, the first three terms of the Weyl expansion are [21]

$$\overline{\rho}_1(\epsilon)=\left(\frac{\alpha\mathcal{A}}{4\pi}-\frac{\sqrt{\alpha}}{8\pi}\frac{\mathcal{L}}{\sqrt{\epsilon}}\right)\theta(\epsilon)+\mathcal{K}\delta(\epsilon)+\cdots, \tag{3}$$

where $\alpha=2m/\hbar^2$, $\mathcal{A}$ is the area, $\mathcal{L}$ is the perimeter, and

$$\mathcal{K}=\frac{1}{12\pi}\oint dl\,\kappa(l)+\frac{1}{24\pi}\sum_i\frac{\pi^2-\theta_i^2}{\theta_i} \tag{4}$$

is the average curvature integrated along the boundary with corrections due to corners with angles θ_i. The oscillating part is obtained from semiclassical periodic orbit theory, and in particular the various trace formulas for $\widetilde{\rho}_1(\epsilon)$ of the form [5]

$$\widetilde{\rho}_1(\epsilon)\approx\frac{1}{\pi\hbar}\sum_\Gamma A_\Gamma(\epsilon)\cos\left(\frac{1}{\hbar}S_\Gamma(\epsilon)-\sigma_\Gamma\frac{\pi}{2}\right). \tag{5}$$

Γ denotes topologically distinct periodic orbits and $S_\Gamma(\epsilon)$ is the classical action integral along the orbit Γ. The amplitude $A_\Gamma(\epsilon)$ depends on energy, the period of the corresponding primitive orbit, the stability of the orbit, and whether it is isolated or nonisolated. The index σ_Γ depends on the topological properties of each orbit. For isolated orbits, it is just the Maslov index. For nonisolated orbits, there may be additional phase factors in the form of odd multiples of $\pi/4$ which we account for, in a slight abuse of notation, by allowing σ_Γ to be half-integer. In the case of nonisolated orbits, Γ denotes distinct families of degenerate orbits. The amplitude of an isolated orbit is given by the Gutzwiller trace formula [1]

$$A_\Gamma(\epsilon)=\frac{T_\gamma(\epsilon)}{\sqrt{|\det(\tilde{M}_\Gamma-I)|}}, \tag{6}$$

where $T_\gamma(\epsilon)$ is the period of the primitive orbit γ, corresponding to Γ (i.e., Γ is an integer repetition of γ) and $\tilde{M}_\Gamma$ is the stability matrix of that orbit.

B. Quantum two-particle density-of-states

Suppose we have a system of two identical noninteracting particles. The total Hamiltonian is the sum of the single-particle Hamiltonians and it follows that the energies of the composite system are just the sums of the single-particle energies. The analog of Eq. (1) is then

$$\rho_2(E)=\sum_{i,j}\delta[E-(\epsilon_i+\epsilon_j)]. \tag{7}$$

A useful relation is that the two-particle density-of-states is the autoconvolution of the single-particle density-of-states:

$$\rho_2(E)=\int_0^E d\epsilon\,\rho_1(\epsilon)\rho_1(E-\epsilon)=\rho_1*\rho_1(E), \tag{8}$$

as can be verified by direct substitution. In fact, this works even if the particles are not identical, where the full density is still the convolution of the two distinct single-particle densities. This would also apply to a single particle in a separable potential, which is mathematically equivalent. Rather than encumber the notation to explicitly allow for this possibility, we defer this discussion to Appendix A, where some formulas for nonidentical, noninteracting particles are presented.

We can decompose the two-particle density-of-states for a system of two identical particles into a symmetric and an antisymmetric density,

$$\rho_2(E)=\rho_S(E)+\rho_A(E). \tag{9}$$

We shall use the terms symmetric/antisymmetric and bosonic/fermionic interchangeably. Each partial density may be obtained using a projection operator onto the relevant subspaces resulting in

$$\rho_{S/A}(E)=\frac{1}{2}\left[\rho_2(E)\pm\frac{1}{2}\rho_1\left(\frac{E}{2}\right)\right]. \tag{10}$$

We seek semiclassical approximations to these quantum expressions, a topic which is pursued in the following sections.

III. SEMICLASSICAL CALCULATIONS FOR THE TWO-PARTICLE SYSTEM

Decomposing the single-particle density into its smooth and oscillatory components as in Eq. (2) gives a decomposition of the two-particle density-of-states into three distinct contributions,

$$\rho_2^{\mathrm{sc}}(E)=\overline{\rho}_1*\overline{\rho}_1(E)+2\overline{\rho}_1*\widetilde{\rho}_1(E)+\widetilde{\rho}_1*\widetilde{\rho}_1(E). \tag{11}$$

The first term is a smooth function of energy since the convolution of two smooth functions results in a smooth function. This is followed by a cross term and finally by a purely oscillating term. The cross term is also an oscillating function. At first, this may seem incorrect since the convolution of a smooth function with an oscillating function usually yields a smooth function. As we will show, the oscillatory nature of the cross term is due to contributions from the end points of the convolution integral. Physically, the smooth term does not depend on dynamics since it corresponds to the Weyl formula in the full two-particle space. The cross

term depends only on single-particle dynamics because it corresponds to the situation where one particle is stationary and the other particle is evolving dynamically on a periodic orbit. It is only the last term that contains two-particle dynamics in the sense that both particles are evolving dynamically on periodic orbits. Hence, we will refer to the last term as the dynamical term.

We find a general expression for $\tilde{\rho}_1 * \tilde{\rho}_1(E)$ by substituting a generalized trace formula for $\tilde{\rho}_1$ and then evaluating the resulting convolution integral using stationary phase asymptotics. Using Eq. (5), the dynamical term can be written as

$$\tilde{\rho}_1 * \tilde{\rho}_1(E) \approx \frac{1}{(\pi\hbar)^2} \sum_{\Gamma_1,\Gamma_2} \int_0^E d\epsilon\, A_{\Gamma_1}(\epsilon) A_{\Gamma_2}(E-\epsilon) \times \cos\left(\frac{1}{\hbar} S_{\Gamma_1}(\epsilon) - \sigma_{\Gamma_1}\frac{\pi}{2}\right) \times \cos\left(\frac{1}{\hbar} S_{\Gamma_2}(E-\epsilon) - \sigma_{\Gamma_2}\frac{\pi}{2}\right). \tag{12}$$

To evaluate this asymptotically, we should include all critical points in the integration domain. Specifically, this integral has a stationary phase point within the integration domain and finite valued end points. We shall show that the stationary phase point corresponds to the situation where both particles are evolving dynamically with the energy partitioned between the two particles in a prescribed way. The end point contributions must be evaluated at energies such that one of the particles has all of the energy while the other has no energy. However, this contradicts our assumption that both particles are evolving—this is the definition of the dynamical term. Moreover, if we were to evaluate this contribution, the result would be meaningless since it involves using the trace formula at zero energy where it is known to fail. So we shall omit the contributions from the end points; this is discussed more fully in Sec. IV D and in Appendix B, as well as in Ref. [22].

Hence, we evaluate the integral in Eq. (12) using only the stationary phase point. To leading order, we can extend the integration limits over an infinite domain. Writing the cosine functions as complex exponentials yields four integrals; the first is

$$\int_{-\infty}^{\infty} d\epsilon A_{\Gamma_1}(\epsilon) A_{\Gamma_2}(E-\epsilon) \exp\left(\frac{i}{\hbar}[S_{\Gamma_1}(\epsilon) + S_{\Gamma_2}(E-\epsilon)]\right) \approx A_{\Gamma_1}(E_0) A_{\Gamma_2}(E-E_0) \times \sqrt{\frac{2\pi\hbar}{|\Upsilon(\Gamma_1,\Gamma_2,E_0)|}} \times \exp\left(\frac{i}{\hbar}[S_{\Gamma_1}(E_0) + S_{\Gamma_2}(E-E_0)] + i\nu\frac{\pi}{4}\right), \tag{13}$$

where

$$\Upsilon(\Gamma_1,\Gamma_2,E_0) = \left(\frac{\partial^2 S_{\Gamma_1}(\epsilon)}{\partial\epsilon^2} + \frac{\partial^2 S_{\Gamma_2}(E-\epsilon)}{\partial\epsilon^2}\right)\Bigg|_{E_0},$$

$$\nu = \mathrm{sign}[\Upsilon(\Gamma_1,\Gamma_2,E_0)]. \tag{14}$$

E_0 is determined from the stationary phase condition

$$\left(\frac{\partial S_{\Gamma_1}(\epsilon)}{\partial\epsilon} + \frac{\partial S_{\Gamma_2}(E-\epsilon)}{\partial\epsilon}\right)\Bigg|_{E_0} = 0 \Rightarrow T_{\Gamma_1}(E_0) = T_{\Gamma_2}(E-E_0), \tag{15}$$

where we have used the fact that the derivative of the action with respect to energy is the period. E_0 is the energy of particle 1, $E-E_0$ is the energy of particle 2, and E is the total energy of the composite system. The saddle energy E_0 has a precise physical interpretation; Eq. (15) says that the energies of the two particles are partitioned so that the periods of both periodic orbits are the same. In other words, at E_0, we have orbits that are periodic in the full two-particle phase space since after the period T, *both* particles return to their initial conditions.

The next integral has the same stationary phase condition as the first integral and is its complex conjugate. The third integral is

$$\int_{-\infty}^{\infty} d\epsilon A_{\Gamma_1}(\epsilon) A_{\Gamma_2}(E-\epsilon) \exp\left(-\frac{i}{\hbar}[S_{\Gamma_1}(\epsilon) - S_{\Gamma_2}(E-\epsilon)]\right) \tag{16}$$

and has no stationary phase point since setting the first derivative of the action to zero yields the stationary phase condition

$$T_{\Gamma_1}(E_0) = -T_{\Gamma_2}(E-E_0). \tag{17}$$

The trace formula only involves orbits with positive period, so we ignore this possibility. The last integral is the complex conjugate of the third and will also be ignored.

Adding the contributions from the first two integrals, we arrive at the two-particle trace formula:

$$\tilde{\rho}_1 * \tilde{\rho}_1(E) \approx \frac{2}{(2\pi\hbar)^{3/2}} \sum_{\Gamma_1,\Gamma_2} \frac{A_{\Gamma_1}(E_0) A_{\Gamma_2}(E-E_0)}{\sqrt{|\Upsilon(\Gamma_1,\Gamma_2,E_0)|}} \times \cos\left(\frac{1}{\hbar}[S_{\Gamma_1}(E_0) + S_{\Gamma_2}(E-E_0)] - (\sigma_{\Gamma_1} + \sigma_{\Gamma_2})\frac{\pi}{2} + \nu\frac{\pi}{4}\right). \tag{18}$$

This result possesses the intuitive properties that, other than factors arising from the stationary phase analysis, the actions and Maslov indices are additive and the amplitudes are multiplicative. We note that this saddle-point analysis fails for the harmonic oscillator, where $\Upsilon = 0$. This is because the two-particle harmonic oscillator has a higher degree of symmetry than we are accounting for here. This is a nongeneric property specific to the harmonic oscillator. We also stress

that we have made no assumption about the stability or structure of the orbits. They can be isolated, stable or unstable or come in families. There are also problems with coexisting isolated orbits and families, such as those of the equilateral triangle billiard [23,5].

Note that the overall $\hbar$ dependence is not multiplicative but picks up an additional factor of $\hbar^{1/2}$ from the stationary phase integral. For isolated orbits, the amplitudes A are independent of $\hbar$ and the expression (18) has a $1/\hbar^{3/2}$ prefactor as opposed to the $1/\hbar$ prefactor of the single-particle trace formula (5). The fact that the $\hbar$ dependence is different implies that the periodic orbits of the full system come in continuous degenerate families rather than isolated trajectories, which in turn implies that there exists a continuous symmetry in the problem [24]. This is an important point which we will address in a companion paper [20]. (It was also noted in Ref. [17].) Nonetheless, it may be helpful to give a brief explanation here. Imagine the full phase-space periodic orbit Γ consists of particle 1 on a periodic orbit Γ_1 with energy E_0 and particle 2 on a distinct periodic orbit Γ_2 with energy $E-E_0$. We can define $t=0$ to be when particle 2 is at some prescribed point on Γ_2. Keeping particle 2 fixed, we can change the position of particle 1 on Γ_1 to generate the initial condition of a distinct but congruent periodic orbit in the full phase space. Continuous time translation of the initial condition on Γ_1 generates a continuous family of congruent periodic orbits in the full phase space. Since the time translational symmetry can be characterized by a single independent symmetry parameter, the $\hbar$ dependence is $O(1/\sqrt{\hbar})$ stronger than for a system with isolated periodic orbits [24,5].

IV. TWO-PARTICLE QUANTUM BILLIARDS

Billiards are two-dimensional enclosures that constrain the motion of a free particle. Classically, a particle has elastic collisions with the walls and depending on the geometric properties of the domain, the dynamics are either regular or chaotic. We study billiard systems containing two noninteracting particles. We ignore the possibility of the particles colliding since such an event would constitute an interaction. This can be conceptualized by thinking of the particles as pure point objects.

In a billiard system, classical orbits possess simple scaling properties. For instance, the action of an orbit Γ, $S_\Gamma(\epsilon)=\sqrt{2m\epsilon}L_\Gamma$ and the period of the orbit is

$$T_\Gamma(\epsilon)=\frac{\partial S_\Gamma(\epsilon)}{\partial\epsilon}=\frac{\sqrt{2m}L_\Gamma}{2\sqrt{\epsilon}}=\frac{\hbar\sqrt{\alpha}}{2\sqrt{\epsilon}}L_\Gamma. \tag{19}$$

The parameter $\alpha=2m/\hbar^2$ already appeared in Eq. (3); it will recur often. For example, the combination αE occurs in all final expressions; this is a result of the scaling property (the quantity αE having the units of 1/length^2). In the theoretical development, it will be convenient to retain α and use it to keep track of relative orders in the semiclassical expansions (since it contains $\hbar$). However, once we have the final expressions, we are free to set it to unity for the purposes of numerical comparisons.

We also mention that for billiards, it is common to express the density-of-states in terms of the wave number k, where $\epsilon=k^2/\alpha$ so that $\rho(k)=2k\rho(\epsilon)/\alpha$. This is convenient since k is conjugate to the periodic orbit lengths L. Therefore, our numerical results will be quoted as a function of k, although it should be stressed that all convolution integrals must be done in the energy domain. Thus, we shall write

$$\rho_2^{\rm sc}(k)=(\overline{\rho}_1*\overline{\rho}_1)(k)+2(\overline{\rho}_1*\widetilde{\rho}_1)(k)+(\widetilde{\rho}_1*\widetilde{\rho}_1)(k). \tag{20}$$

Here, it is understood that each of the functions in brackets is first evaluated in the energy domain and then converted to the k domain through the Jacobian relation above. This will always be the case when the argument is k, so that we will not always write brackets around the various functions. In terms of the wave number k, the decomposition (10) becomes

$$\rho_{S/A}(k)=\frac{1}{2}\left[\rho_2(k)\pm\frac{1}{\sqrt{2}}\rho_1\left(\frac{k}{\sqrt{2}}\right)\right]. \tag{21}$$

A. Smooth term

The smooth part is defined by the convolution integral

$$\overline{\rho}_1*\overline{\rho}_1(E)=\int_0^E d\epsilon\,\overline{\rho}_1(\epsilon)\overline{\rho}_1(E-\epsilon), \tag{22}$$

where $\overline{\rho}_1$ is given by the Weyl expansion. The expansion in Eq. (3) is taken only to order $\hbar^0$. Hence, after expanding the integrand in Eq. (22), it is formally meaningless to include terms that are $O(1/\hbar)$ since there are corrections of the same order in $\hbar$ that have not been calculated. Ignoring these terms and performing the necessary integrations, the smooth term is found to be

$$\overline{\rho}_1*\overline{\rho}_1(E)\approx\frac{\alpha^2\mathcal{A}^2}{16\pi^2}E-\frac{\alpha^{3/2}\mathcal{A}L}{8\pi^2}\sqrt{E}+\frac{\alpha\mathcal{L}^2}{64\pi}+\frac{\alpha\mathcal{A}K}{2\pi}. \tag{23}$$

B. Cross term

We next convolve $\overline{\rho}_1$ term by term with $\widetilde{\rho}_1$. Asymptotically, each convolution integral receives contributions from the upper and lower end points. However, we shall only include one of these, namely, the end point for which the trace formula is not evaluated at zero energy. We neglect the other end point for reasons explained in Sec. IV D and Ref. [22]. This is also discussed in Appendix B, where we evaluate the various integrals for the cross term exactly using isolated billiard orbits and show explicitly that an appropriate asymptotic expansion of the exact expression leads to consistent results.

After convolution, we find the area term involves the integral

$$\mathrm{Re}\left\{ \int_0^E d\epsilon A_\Gamma(E-\epsilon)\exp\left(i\sqrt{\alpha(E-\epsilon)}L_\Gamma - i\sigma_\Gamma\frac{\pi}{2}\right)\right\}. \tag{24}$$

The lower end point $\epsilon=0$ corresponds to the physically meaningful situation while the upper end point is spurious in the sense mentioned above and discussed in detail below. Hence, to leading order, we can remove the amplitude factor from inside the integral, Taylor expand the argument of the exponential, and extend the upper limit to infinity. This leads to

$$I_{\mathcal{A}}(E)\approx\frac{\alpha\mathcal{A}}{4\pi^2}\sum_\Gamma\frac{A_\Gamma}{T_\Gamma}\cos\left(\Theta_\Gamma-\frac{\pi}{2}\right), \tag{25}$$

where $\Theta_\Gamma=\sqrt{\alpha E}L_\Gamma-\sigma_\Gamma(\pi/2)$. By similar logic, the perimeter and curvature terms are

$$I_{\mathcal{L}}(E)\approx-\frac{\sqrt{\alpha}\mathcal{L}}{8\pi^{3/2}\sqrt{\hbar}}\sum_\Gamma\frac{A_\Gamma}{\sqrt{T_\Gamma}}\cos\left(\Theta_\Gamma-\frac{\pi}{4}\right),$$
$$I_{\mathcal{K}}(E)\approx\frac{\mathcal{K}}{\pi\hbar}\sum_\Gamma A_\Gamma\cos(\Theta_\Gamma). \tag{26}$$

Note that all amplitudes and periods in Eqs. (25) and (26) are evaluated at the system energy E. Recall $\alpha\propto 1/\hbar^2$ so that after convolution the sequence is an expansion in powers of $\sqrt{\hbar}$ and not in powers of $\hbar$ as for the original Weyl series (3). We also note that the first correction to $I_{\mathcal{A}}$ may be of the same order as $I_{\mathcal{K}}$ (as happens for the disk [25]) and should be included if this is the case. We then have

$$\overline{\rho_1}*\widetilde{\rho}_1(E)\approx I_{\mathcal{A}}(E)+I_{\mathcal{L}}(E)+I_{\mathcal{K}}(E). \tag{27}$$

C. Dynamical term

As an application of the two-particle trace formula (18), we now derive a general expression for the dynamical term that is valid for any billiard problem. To this end, the first task is to determine the saddle energy from the stationary phase condition. Inserting Eq. (19) into Eq. (15) yields

$$\frac{L_{\Gamma_1}}{\sqrt{E_0}}=\frac{L_{\Gamma_2}}{\sqrt{E-E_0}}, \tag{28}$$

which implies

$$\frac{E_0}{E}=\frac{L_{\Gamma_1}^2}{L_{\Gamma_1}^2+L_{\Gamma_2}^2},\quad \frac{E-E_0}{E}=\frac{L_{\Gamma_2}^2}{L_{\Gamma_1}^2+L_{\Gamma_2}^2} \tag{29}$$

and

$$\Upsilon(\Gamma_1,\Gamma_2,E_0)=-\sqrt{\frac{2m}{4E^{3/2}}}\frac{(L_{\Gamma_1}^2+L_{\Gamma_2}^2)^{5/2}}{L_{\Gamma_1}^2L_{\Gamma_2}^2}. \tag{30}$$

Clearly $\nu=-1$. We then substitute these results into Eq. (18) to obtain the two-particle trace formula for billiards

$$\widetilde{\rho}_1*\widetilde{\rho}_1(E)\approx\frac{4E^{3/4}}{\sqrt{\hbar}\alpha^{1/4}(2\pi\hbar)^{3/2}}\times\sum_{\Gamma_1,\Gamma_2}\frac{L_{\Gamma_1}L_{\Gamma_2}}{(L_{\Gamma_1}^2+L_{\Gamma_2}^2)^{5/4}}A_{\Gamma_1}(E_0)A_{\Gamma_2}(E-E_0)\times\cos\left(\sqrt{\alpha E}\sqrt{L_{\Gamma_1}^2+L_{\Gamma_2}^2}-(\sigma_{\Gamma_1}+\sigma_{\Gamma_2})\frac{\pi}{2}-\frac{\pi}{4}\right). \tag{31}$$

If the single-particle periodic orbits are not isolated, then one must make direct use of the corresponding single-particle amplitudes in Eq. (5) evaluated at the appropriate energies. We will show an explicit example of this when we analyze the disk billiard. Since the amplitudes A_Γ typically have an energy dependence, one cannot make any general statements about the energy dependence of this term except that the greater the dimensionality of the periodic orbit families, the greater the energy prefactor. For example, for the disk, it turns out to be $E^{1/4}$.

If the single-particle periodic orbits are isolated, the amplitudes are given by Eq. (6), which for billiards is

$$A_\Gamma(\epsilon)=\frac{\hbar\sqrt{\alpha}}{2\sqrt{\epsilon}}\frac{L_\gamma}{\sqrt{|\det(\tilde{M}_\Gamma-I)|}}. \tag{32}$$

In this case, the Gutzwiller amplitudes are evaluated at E_0 and $E-E_0$, so we again make use of Eq. (29). After some algebra and simplification, we find

$$\widetilde{\rho}_1*\widetilde{\rho}_1(E)\approx\frac{\alpha^{3/4}}{(2\pi)^{3/2}E^{1/4}}\times\sum_{\Gamma_1,\Gamma_2}\frac{L_{\gamma_1}L_{\gamma_2}(L_{\Gamma_1}^2+L_{\Gamma_2}^2)^{-1/4}}{\sqrt{|\det(\tilde{M}_{\Gamma_1}-I)||\det(\tilde{M}_{\Gamma_2}-I)|}}\times\cos\left[\sqrt{\alpha E}\sqrt{L_{\Gamma_1}^2+L_{\Gamma_2}^2}-(\sigma_{\Gamma_1}+\sigma_{\Gamma_2})\frac{\pi}{2}-\frac{\pi}{4}\right]. \tag{33}$$

Note the $E^{-1/4}$ prefactor, which implies the amplitude, decays weakly with energy. This is the same prefactor that occurs in the single-particle trace formula of the disk. This is not a coincidence, but arises from the fact that in both problems, the periodic orbits come in one parameter families. In formula (33), one must be careful to distinguish between L_Γ, the length of a periodic orbit and L_γ, the length of the corresponding primitive periodic orbit. In general $L_\Gamma=n_\Gamma L_\gamma$ where n_Γ is the repetition index of that orbit.

D. Spurious end-point contributions

As mentioned above, when confronted with convolution integrals, it is natural to analyze them asymptotically. This involves identifying the critical points and doing appropriate expansions in their neighborhoods. In our paper, these critical points are either stationary phase points or end points. The power of semiclassical methods is that each critical point can be given an immediate physical interpretation. For example, the stationary phase point in the dynamical term is found to be that energy such that the two particles have the same period so that the motion is periodic in the full two-particle phase space. This is intuitively reasonable. However, the same integral also has end points with finite valued contributions. We could do an asymptotic calculation in the vicinity of these points, but we can argue immediately that the result is spurious and not physically meaningful.

Recall the trace formulas are asymptotic in $\hbar$, which typically also means asymptotic in energy. At the end points, one of the trace formulas is evaluated at small energy where it is known to be invalid. Alternatively, we can substitute for the trace formula any expression that is asymptotically equivalent to it and expect all meaningful results to be invariant to leading order. If we do this, we will find the end point contribution changes while the stationary phase contribution remains invariant, to leading order.

A further argument is that the structure of the end point contribution will be incorrect. Typically, it will be a sinusoid with an argument that does not depend on energy, but only depends on the properties of one of the orbits. Hence, it will have the same asymptotic structure as the cross term. However, we know that the cross term completely describes all such contributions and any further contribution with the same structure must be spurious.

Similarly, when we evaluate the cross term, we have two end point contributions. At one of these, we are evaluating the trace formula at some finite energy, which is reasonable. This end point corresponds to orbits that are periodic in the full phase space and in which one particle evolves on a single-particle periodic orbit with all the energy, while the other remains fixed at some point in phase space with zero energy. At the other end point, we are evaluating the trace formula at zero energy, which is problematic. This corresponds to the contradictory situation in which the evolving particle has zero energy while the fixed particle has all the energy. In addition, upon inspection of this end point contribution, we find a function that is not oscillatory in energy and therefore has the same asymptotic structure as the smooth term. However, the smooth term already completely describes the average behavior of the two-particle density-of-states and any further contributions with the same structure must be spurious.

These situations are further examples of a general situation described in Ref. [22] where it was shown that when integrating over the trace formula to obtain physical quantities, one should include all critical points except ones at which the trace formula is evaluated at zero energy. Such contributions should simply be ignored as spurious. In Ref. [22], the application was to thermodynamic calculations, but the principle is precisely the same. In Appendix B, we show the result of evaluating the cross term exactly for isolated orbits. An asymptotic analysis of this result leads to two terms that we can identify as coming from the two end points. One has the form used in this paper while the other is clearly spurious.

V. TWO-PARTICLE DISK BILLIARD

In this section, we apply our results to the problem of two identical noninteracting particles moving in a two-dimensional disk of radius R. Quantum mechanically, this problem is a simple extension of the one-body problem. Nevertheless, the spectrum has some interesting features that we discuss below.

A. Quantum mechanics

For the disk billiard, a general two-particle state can be written as

$$|m_1\, n_1, m_2\, n_2\rangle = |m_1\, n_1\rangle \otimes |m_2\, n_2\rangle, \tag{34}$$

where the azimuthal quantum numbers m_1, $m_2 = 0, \pm 1, \pm 2, \ldots$ and the radial quantum numbers n_1, $n_2 = 1,2,3, \ldots$. We shall also use a more compact notation $|N_1, N_2\rangle = |m_1\, n_1, m_2\, n_2\rangle$ where N denotes a pair of integers (m,n). We can immediately write down the wave numbers of the two-particle system as

$$k_{N_1 N_2} = \sqrt{\left(\frac{Z_{N_1}}{R}\right)^2 + \left(\frac{Z_{N_2}}{R}\right)^2}, \tag{35}$$

where Z_N denotes the nth zero of the mth Bessel function $J_m(z)$. The set of all two-particle states is given by $\{|N_1, N_2\rangle\}$.

The spectrum is highly degenerate. A typical state $|N_1, N_2\rangle$ is eightfold degenerate since we can reverse the sign of either m_1 or m_2 or interchange the two particles and the resultant state has the same energy. However, if either m_1 or m_2 is zero or if $N_1 = N_2$ $(m \neq 0)$ then the state is fourfold degenerate. If $m_1 = m_2 = 0$ and $N_1 \neq N_2$, then the state is twofold degenerate whereas if $m_1 = m_2 = 0$ and $N_1 = N_2$, then the state is nondegenerate. If the particles are in distinct states, the degenerate multiplets divide evenly between the symmetric and antisymmetric spaces. However, if the particles are in the same state, $N_1 = N_2$, it is somewhat less trivial. If $N_1 = N_2$ and $m_1 = m_2 \neq 0$, there is a fourfold degenerate set of states: $|m\, n, m\, n\rangle$, $|-m\, n, -m\, n\rangle$, $|m\, n, -m\, n\rangle$, and $|-m\, n, m\, n\rangle$. The first two states belong to the symmetric space. From the second two states, we can construct one symmetric and one antisymmetric combination. (This is analogous to coupling two spin 1/2 states to construct a threefold symmetric $S = 1$ state and a nondegenerate antisymmetric $S = 0$ state.) If $N_1 = N_2$ and $m_1 = m_2 = 0$, this yields the state $|0\, n, 0\, n\rangle$, which is singly degenerate and belongs to the symmetric space.

The quantum density-of-states

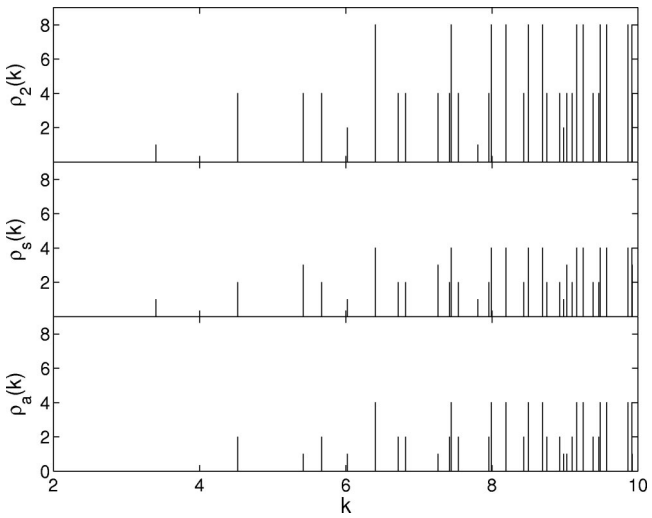

FIG. 1. (Top) The quantum density-of-states for two identical particles in the disk billiard. (Middle) Bosonic density-of-states. (Bottom) Fermionic density-of-states. In each case, the heights indicate the degeneracy of the state.

$$\rho_2(k)=\sum_{N_1,N_2}\delta(k-k_{N_1N_2}) \tag{36}$$

and the corresponding symmetric and antisymmetric densities are shown in Fig. 1 as a function of the wave number k. Note that in this figure some of the peaks have different degeneracies in the symmetric and antisymmetric densities, as discussed above.

B. Semiclassical density-of-states

We first review the semiclassical decomposition of the single-particle density-of-states. The smooth part of the density-of-states may be obtained using the general result for two-dimensional billiards (3). In fact, many higher-order terms have been calculated [7]. But, for our purposes, it suffices to use the first three terms as in Eq. (3) with $\mathcal{A}=\pi R^2$, $\mathcal{L}=2\pi R$, and $\mathcal{K}=1/6$.

The oscillating part of the level density can be obtained using trace formulas for systems with degenerate families of orbits. The periodic orbit families may be uniquely labeled by two integers (v,w), where v is the number of vertices and w is the winding number around the center. The two integers must satisfy the relation $v\geqslant 2w$. The length of an orbit with vertex number v and winding number w is given by $L_{vw}=2vR\sin(\pi w/v)$. With this notation, the trace formula for the oscillating part of the density-of-states is [26]

$$\tilde{\rho}_1(\epsilon)\approx\frac{\alpha^{3/4}}{2\sqrt{2\pi}\epsilon^{1/4}}\sum_{vw}\frac{\mathcal{D}_{vw}L_{vw}^{3/2}}{v^2}\cos\left(\sqrt{\alpha E}L_{vw}-3v\frac{\pi}{2}+\frac{\pi}{4}\right), \tag{37}$$

where the sum goes from $w=1,\ldots,\infty$ and $v=2w,\ldots,\infty$ and the degeneracy factor $\mathcal{D}_{vw}$, which accounts for negative windings, is 1 for $v=2w$ and 2 for $v>2w$. Comparing Eq. (37) with the general form (5), we identify

$$A_{vw}(\epsilon)=\frac{\sqrt{2\pi}\alpha^{3/4}\hbar\mathcal{D}_{vw}L_{vw}^{3/2}}{4v^2\epsilon^{1/4}},$$

$$\sigma_{vw}=3v-\tfrac{1}{2}. \tag{38}$$

Adding the smooth and oscillating terms gives the semiclassical approximation to the single-particle density-of-states which we denote by $\rho_1^{sc}(\epsilon)$.

To evaluate the semiclassical approximation to the two-particle density-of-states, we must evaluate the smooth, cross, and dynamical terms. The smooth term can be taken from Eq. (23) to be

$$\overline{\rho_1}*\overline{\rho_1}(E)\approx\frac{\alpha^2R^4}{16}E-\frac{\alpha^{3/2}R^3}{4}\sqrt{E}+\left(\frac{3\pi+4}{48}\right)\alpha R^2. \tag{39}$$

The arguments of the previous section and in particular Eqs. (25), (26), and (27) lead to the cross term

$$\begin{aligned}\overline{\rho_1}*\tilde{\rho}_1(E)\approx&\frac{\alpha^{5/4}R^2E^{1/4}}{4\sqrt{2\pi}}\\&\times\sum_{vw}\frac{\sqrt{L_{vw}}\mathcal{D}_{vw}}{v^2}\left[\cos\left(\Phi_{vw}-\frac{\pi}{2}\right)\right.\\&-\sqrt{\frac{\pi}{2}}\chi_{vw}\cos\left(\Phi_{vw}-\frac{\pi}{4}\right)\\&\left.+\left(\frac{1}{3}+\frac{R^2}{2L_{vw}^2}\right)\chi_{vw}^2\cos\Phi_{vw}\right],\end{aligned} \tag{40}$$

where $\Phi_{vw}=\sqrt{\alpha E}L_{vw}-3v\pi/2+\pi/4$ and $\chi_{vw}=\sqrt{L_{vw}}/(\alpha E)^{1/4}R$. We have also included the first correction to the area term $I_{\mathcal{A}}(E)$, which appears in the third term above [25]. The dynamical term can be obtained using Eq. (31). Noting that Γ_i in Eq. (31) corresponds to the pair of integers (v_i,w_i), the result is

$$\begin{aligned}\tilde{\rho}_1*\tilde{\rho}_1(E)\approx&\frac{\alpha^{5/4}E^{1/4}}{4\sqrt{2\pi}}\sum_{v_1w_1,v_2w_2}\left(\prod_{i=1}^{2}\frac{\mathcal{D}_iL_i^2}{v_i^2}\right)L_{12}^{-3/2}\cos\left[\sqrt{\alpha E}L_{12}\right.\\&\left.-3(v_1+v_2)\frac{\pi}{2}+\frac{\pi}{4}\right],\end{aligned} \tag{41}$$

where $L_i=L_{v_iw_i}$, $\mathcal{D}_i=\mathcal{D}_{v_iw_i}$, and $L_{12}=\sqrt{L_1^2+L_2^2}$.

C. Numerics

For numerical purposes, we take $\alpha=1$ and $R=1$ so the single-particle energies are just the squares of zeros of Bessel functions. Since we can only include a finite number of orbits, the periodic orbit sums must be truncated. As a representative case, we truncate the sum in Eq. (40) at $w_{\max}=50$,$v_{\max}=100$ (see Fig. 2) and use the same limits to truncate the quadruple sum in Eq. (41). This is a relatively small set of orbits, yet it does very well in reproducing the peaks of the quantum density-of-states. As an illustration, we show

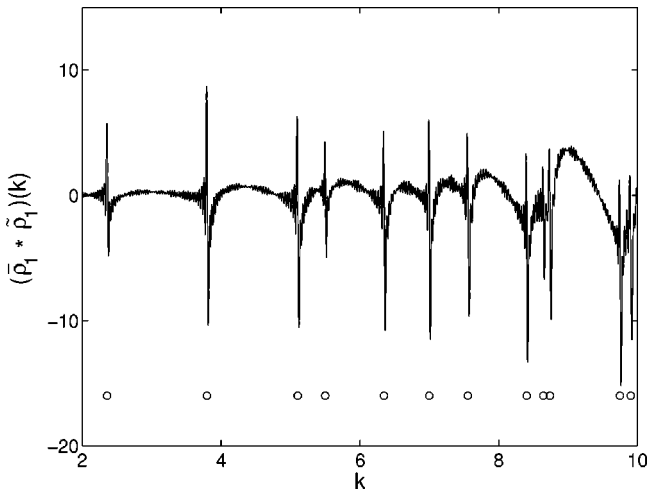

FIG. 2. The cross term (40) of the semiclassical density-of-states for two identical particles in the disk billiard. In this case, we truncate the sum in Eq. (40) at $w_{\max}=50, v_{\max}=100$. The circles indicate the level sequence of the one-body problem obtained from Einstein-Brillouin-Keller (EBK) quantization. Note the kinks that occur at these positions.

the first few peaks of Eq. (20) in Fig. 3. We calculated the semiclassical density-of-states on the interval $0 \leqslant k \leqslant 11$. After doing so, we found only two sets of two peaks that were not resolved. These are shown in Fig. 4. Obviously, using more orbits will produce better results, but this increases the computation time because of the quadruple sum in Eq. (41). (Although one can reduce the computational overhead by limiting the sum to orbits whose amplitude exceeds some prescribed threshold [25].)

As an additional test, we want to determine whether Eq. (20) gives the correct degeneracies. We could do this by

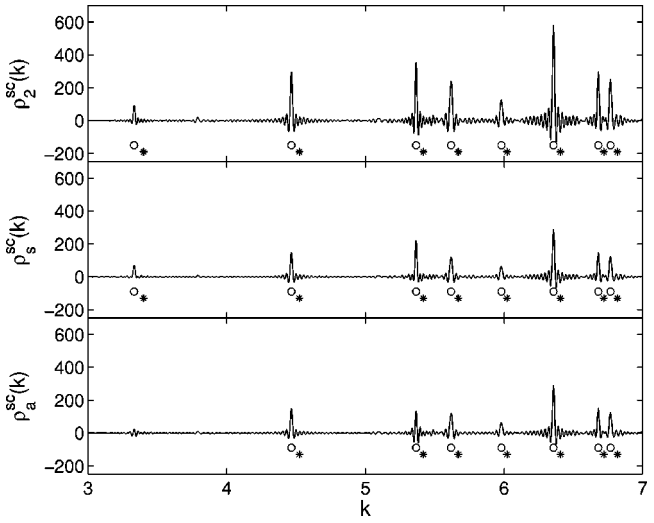

FIG. 3. (Top) The first few peaks of the semiclassical density-of-states (20). (Middle) Semiclassical approximation to the bosonic density-of-states. (Bottom) Semiclassical approximation to the fermionic density-of-states. In each case, the circles and stars represent the appropriate level sequences obtained from EBK quantization and quantum mechanics, respectively. Note the positions of the peaks more closely reproduce the EBK spectrum.

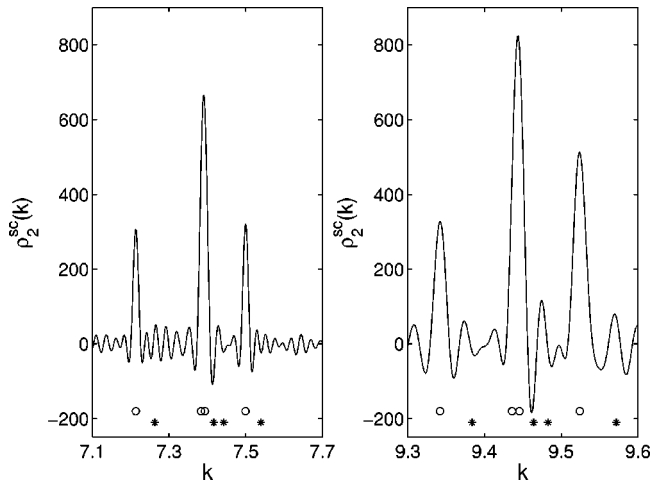

FIG. 4. Two sets of two peaks in the semiclassical density-of-states (20) that are not resolved. (Left) The middle peak is not resolved into the two peaks at $k=7.4163$ (corresponding to the quartet $\{|0\,1,\pm 1\,2\rangle,|\pm 1\,2,0\,1\rangle\}$) and $k=7.4423$ (corresponding to the octet $\{|\pm 1\,1,\pm 3\,1\rangle,|\pm 3\,1,\pm 1\,1\rangle\}$). The corresponding EBK quartet and octet energies occur at $k=7.3831$ and $k=7.3932$, respectively. Note that $\Delta k_{\mathrm{EBK}}=0.0101$ and $\Delta k_{\mathrm{QM}}=0.026$ so that the spacing of the two unresolved levels is smaller in the semiclassical spectrum than in the quantum-mechanical spectrum. (Right) The middle peak is not resolved into the two peaks at $k=9.4641$ (corresponding to the quartet $\{|\pm 1\,1,0\,3\rangle,|0\,3,\pm 1\,1\rangle\}$) and $k=9.4829$ (corresponding to the octet $\{|\pm 3\,1,\pm 1\,2\rangle\}$). The corresponding EBK quartet and octet energies occur at $k=9.4359$ and $k=9.4456$, respectively. Here, $\Delta k_{\mathrm{EBK}}=0.0097$ and $\Delta k_{\mathrm{QM}}=0.0188$.

integrating the area under each of the peaks. However, a simpler procedure is to do a Gaussian smoothing by convolving $\rho_2^{\mathrm{sc}}(k)$ with an unnormalized Gaussian of variance σ:

$$\rho_2^{\mathrm{sc}}(k) * G_\sigma(k) = \int_0^\infty dk' \rho_2^{\mathrm{sc}}(k') G_\sigma(k-k'), \tag{42}$$

where

$$G_\sigma(k) = \exp(-k^2/2\sigma^2) \tag{43}$$

and σ is the smoothing width. The reason for this is that if the variance σ of the Gaussian is larger than the intrinsic width of a peak in the semiclassical spectrum, then each peak acts like $D\delta(k-k_n)$ with respect to the Gaussian. Thus, the integral in Eq. (42) becomes $DG_\sigma(k-k_n)$ or D at $k=k_n$. Of course, this is invalid when the spacing between two adjacent peaks is smaller than about σ. Some examples are discussed in the next section.

We also studied the symmetrized densities by using expression (21) for both the quantum and semiclassical densities and then convolving as above. The periodic orbit sums in the oscillating parts of the one- and two-body densities were truncated in the standard manner as before. The result of this numerical procedure is shown in Fig. 5. Clearly, the semiclassical approximations reproduce the correct degeneracies of the quantum spectrum as well as the approximate positions.

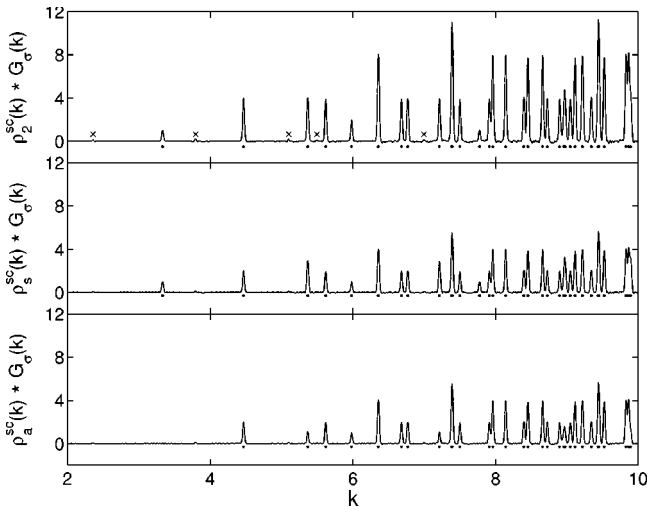

FIG. 5. (Top) The smoothed semiclassical density-of-states obtained from numerical convolution of Eq. (20) with Eq. (43). Note the artifacts of the single-particle EBK spectrum, which occur at the positions marked by an ''X.'' (Middle) The smoothed semiclassical bosonic density-of-states obtained from numerical convolution of Eq. (21) (with the + sign) and Eq. (43). (Bottom) The smoothed semiclassical fermionic density-of-states obtained from numerical convolution of Eq. (21) (with the − sign) and Eq. (43). In each case the sequence of dots represent the corresponding EBK spectrum and $\sigma = 0.0125$.

D. Discussion

In Ref. [26], it was noted that the trace formula replicates the single-particle EBK spectrum obtained from torus quantization more precisely than it duplicates the exact single-particle quantum spectrum. After inspection of Figs. 3 and 5, we notice the same effect in the two-particle spectrum. This property of the trace formulas also accounts for the unresolved peaks in the semiclassical spectrum. When the spacing of two levels of the EBK spectrum is very small, our truncated trace formulas may not resolve them, regardless of the spacing of the corresponding levels in the quantum spectrum (cf. Fig. 4).

Comparing Figs. 1 and 5, we observe generally good agreement between the quantum and semiclassical spectra. Still, there are some apparent inconsistencies, for example, the two tall peaks in Fig. 5. These are the two sets of unresolved levels in Fig. 4, in each case, an octet and a quartet. The reason for the discrepancy is the level spacings are smaller than the smoothing width σ, in contradiction to the assumption above, so that the peak height does not equal the degeneracy. In fact, the peak heights observed are rather close to 12 since the octets and quartets are very nearly degenerate on the scale of σ and act almost like a 12-fold degenerate set. It is not perfectly 12 due to the fact that the degeneracy is not perfect. However, we also observe that the integrated weight under the peak is consistent with a set of 12 energy levels.

Other inconsistencies in Fig. 5 occur for the same reason. Of course, overall improvements can be made by including more orbits. However, it is a fundamental problem that an integrable system will have a large number of small spacings, since the spacing distribution has a Poisson character. In fact, even a chaotic system with noninteracting particles would have a Poisson spacing distribution. This is because the separate single-particle energies are constants of motion and when we combine many independent spectra the resulting distribution is Poisson, even if the distributions of the separate spectra are not [27]. One might then wonder if this is a fatal problem in higher dimensions. If one's motivation is to determine gross shell structure, a point of view stressed in Ref. [5], this is not a problem. If one's motivation is to reproduce the full quantum spectrum, one might still argue that it is not really a problem. Any peak has a width associated with it which is related to the number of orbits used in analyzing the trace formula. This width gives a numerical uncertainty to the energy of a multiplet. Even if two peaks are unresolved, the amount of information is essentially the same. We know the number of states involved by integrating under the peak. Also, we know the energy of all those states to the precision of the peak width, just as for resolved peaks. In that sense, we know the energies of unresolved peaks to the same precision as resolved peaks. Either way, the important criterion is that the peak width should be smaller than the mean spacing between states. This problem of unresolved peaks is less of a problem for chaotic systems where we would not typically expect more than two states to be involved in an unresolved multiplet. Also, adding interactions will tend to lift such near degeneracies and reduce this effect.

In Fig. 5 we also observe artifacts of the single-particle spectrum (some examples are marked by an ''X'') which arise from errors in the cross term. These presumably decrease when corrections to the single-particle trace formula are incorporated into the cross term.

These numerical findings support our analytical results. We now test those results in the rather different context of a chaotic billiard.

VI. TWO-PARTICLE CARDIOID BILLIARD

In this section, we study the problem of two identical noninteracting particles evolving in the cardioid billiard, which is fully chaotic [28]. Since the billiard has a reflection symmetry, all the quantum states are either even or odd (this symmetry should not be confused with the symmetry due to particle exchange). In the subsequent analysis, we will exclusively use the odd spectrum. The reason for this is to avoid the additional complication of *diffractive* orbits that strike the vertex. Classically, these orbits are undefined and are therefore not included in the standard Gutzwiller theory. Studies of diffractive effects in trace formulas can be found in Refs. [29] and [30]. The latter reference explores the specific application to the cardioid and shows that diffractive orbits are important in describing the even spectrum but are largely absent from the odd spectrum.

We could proceed as before by doing an explicit semiclassical analysis of each term in the decomposition of the two-particle semiclassical density-of-states (11). However, we can simplify the analysis by removing single-particle dynamics from the discussion. That is, we will focus exclusively on those quantum-mechanical and semiclassical quan-

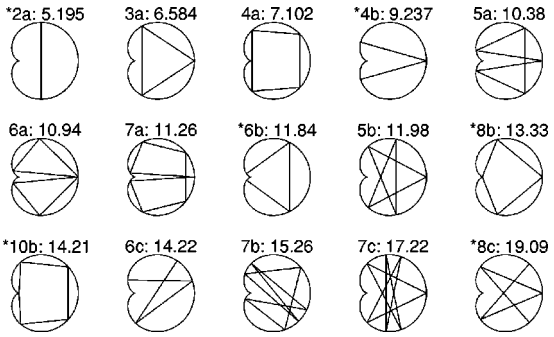

FIG. 6. Some of the shorter periodic orbits of the cardioid in the full domain. The label of each orbit includes the number of reflections and also a letter index to further distinguish it. The asterisk designates a self-dual orbit [30]. The two orbits $*8b$ and $*10b$ reflect specularly near the cusp, contrary to appearances while the orbit $4a$ misses the cusp. From Ref. [30].

tities that inherently describe two-particle dynamics. More specifically, we compare the Fourier transform of the dynamical term

$$\tilde{F}_2^{\mathrm{sc}}(L)=\mathcal{F}\{\tilde{\rho}_1*\tilde{\rho}_1(k)\} \tag{44}$$

with its quantum-mechanical analog which we define to be

$$\tilde{F}_2^{\mathrm{qm}}(L)=\mathcal{F}\{\rho_2(k)-\overline{\rho}_1*\overline{\rho}_1(k)-2\overline{\rho}_1*\tilde{\rho}_1(k)\}. \tag{45}$$

The integral operator $\mathcal{F}$ will be defined precisely below. In the semiclassical transform (44), we use Eq. (33) expressed in terms of the wave number. Here, Γ_1 and Γ_2 are periodic orbits in the fundamental domain (i.e., the half-cardioid) and L_{γ_i} are the primitive lengths of the orbit Γ_i in the fundamental domain. Orbit properties are discussed in Refs. [31] and [30] and some representative orbits are shown in Fig. 6. The stability matrices in the denominator are computed using the standard prescription for the stability of free flight billiards (see, for example, Ref. [4]).

In the quantum-mechanical analog Eq. (45), $\rho_2(k)$ is the quantum two-particle density-of-states, $\rho_2(k)=\Sigma_I\delta(k-k_I)$, where the superindex I denotes the pair of integers (i,j) and $k_I=\sqrt{k_i^2+k_j^2}$. In Eq. (45), we subtract the smooth average part and the part that contains single-particle dynamics. Using $\mathcal{A}=3\pi/4$, $\mathcal{L}=6$, and $\mathcal{K}=3/16$ in Eq. (23) and in Eqs. (25), (26), and (27) yields the smooth and cross terms, respectively. For the cross term, one must also use the periods (19) and amplitudes (32) in Eqs. (25) and (26) evaluated at the system energy E.

A. Numerics for the unsymmetrized cardioid

As before, we take $\alpha=1$ and use a standard sized cardioid as in Ref. [30] to obtain the single-particle spectrum. We numerically compare the two-particle quantum mechanics with the two-particle semiclassics by making a direct comparison of the Fourier transforms in the reciprocal space of orbit lengths, L. In this space, we expect peaks at lengths that correspond to the Euclidean lengths of the *full* periodic orbits of the two-particle system. For instance, if a two-particle

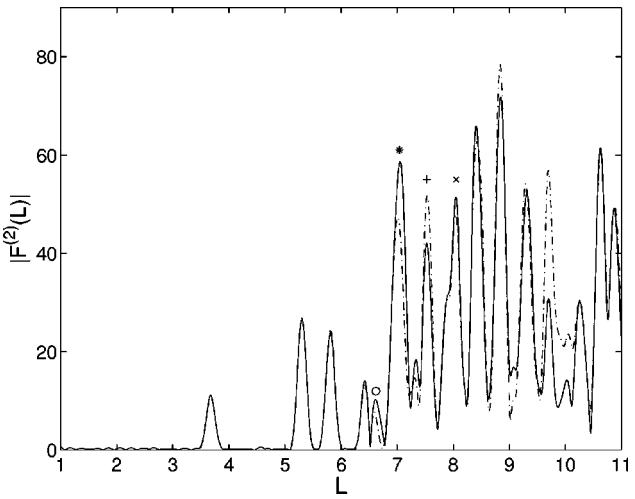

FIG. 7. The Fourier transform of the dynamical part of the two-particle density-of-states. The solid line is the transform of the quantum-mechanical two-particle spectrum Eq. (45) and the dashed-dotted line is the transform of the semiclassical two-particle trace formula Eq. (44). All relevant geometrical periodic orbits with length $L_\Gamma=\sqrt{L_{\Gamma_1}^2+L_{\Gamma_2}^2}<11$ have been included. (Symbols described in the text.)

orbit Γ is comprised of particle 1 traveling on the single-particle orbit Γ_1 and particle 2 traversing a distinct single-particle orbit Γ_2, we expect a peak at $L_\Gamma=\sqrt{L_{\Gamma_1}^2+L_{\Gamma_2}^2}$. In the event that both particles are on the same single-particle orbit Γ, we expect a peak at $\sqrt{2}L_\Gamma$. In this way, any peak in the two-particle spectrum can be attributed to the dynamics of a particular periodic orbit of the full classical phase space.

We construct the two-particle spectrum by adding the energies of the single-particle spectrum. We include the first 1250 single-particle energies which allows us to construct the first 766 794 two-particle energy levels representing all two-particle energies less than 6.8856×10^3.

For a precise numerical comparison, we define the Fourier transform

$$\mathcal{F}\{f(k)\}=\int_{-\infty}^{\infty}dk w(k)e^{ikL}f(k) \tag{46}$$

as a function of the conjugate variable L. Here, $w(k)$ is the three-term Blackman-Harris window function [32]

$$w(k)=\begin{cases}\displaystyle\sum_{j=0}^{2}a_j\cos\left(2\pi j\frac{k-k_0}{k_f-k_0}\right), & k_0<k<k_f,\\ 0, & \text{otherwise,}\end{cases} \tag{47}$$

with $(a_0,a_1,a_2)=(0.423\,23,-0.497\,55,0.079\,22)$. We choose k_0 and k_f so that the window function goes smoothly to zero at the first and last eigenvalues of the two-particle spectrum. Numerical integration of Eqs. (44) and (45) using this definition of $\mathcal{F}$ is displayed in Fig. 7. In the semiclassical transform, a total of 100 periodic orbits (including multiple repetitions) were used.

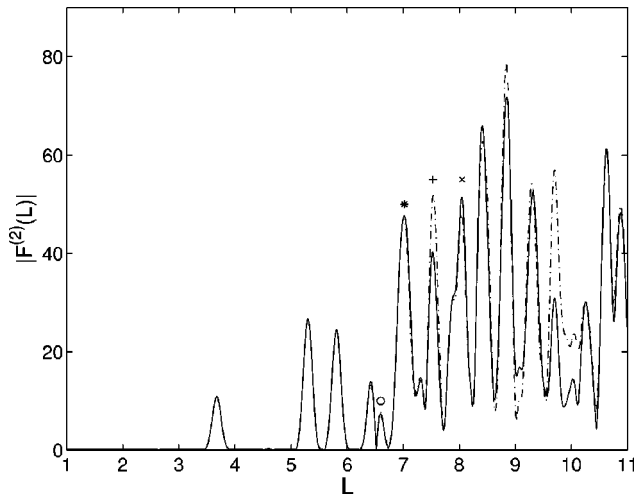

FIG. 8. Same as Fig. 7 except that the cross term in Eq. (45) is computed using single-particle quantum mechanics. (Symbols described in the text.)

In Fig. 7, we observe good agreement between the quantum and semiclassical results for $L<6.5$ and $L>10.3$. In the region $6.5<L<10.3$, there are appreciable discrepancies for the following reason. Recall that the amplitude of the two-particle trace formula (33) applies only to billiard systems whose single-particle periodic orbits are isolated. In the single-particle cardioid problem, there exist orbits that are not well isolated in phase space, in fact, two geometric orbits and a diffractive orbit are sometimes very close in phase space, for example, the two geometric orbits $4a$ and $*10b$ together with the similar looking diffractive orbit $4a'$ (not shown) [30]. In this event, the stationary phase approximation underlying the Gutzwiller formalism fails as does the argument that diffractive orbits do not affect the odd spectrum. As a result, whenever a two-particle orbit in the full space is comprised of one or both particles on one of these problematic single-particle orbits, the resulting two-particle

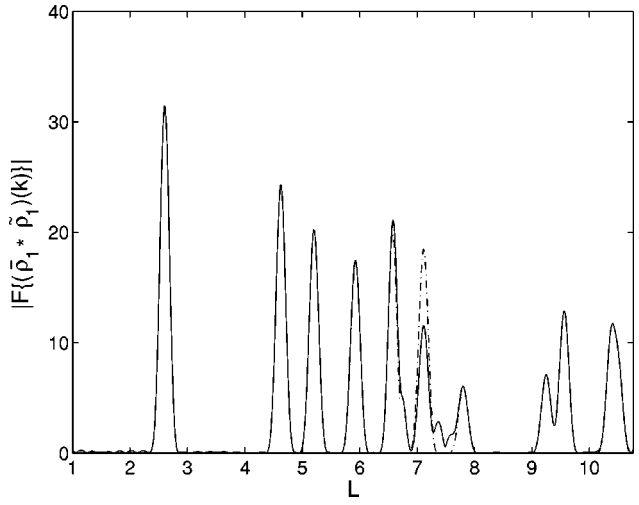

FIG. 9. The Fourier transform of the cross term for the cardioid billiard calculated using quantum mechanics (solid) and periodic orbit theory (dashed dotted).

TABLE I. A few of the periodic orbits that conspire to give trouble around $L=7.6$.

Λ	Γ_1	Γ_2	L_Λ
1	$\frac{1}{2}(*2a)$	$4a$	7.562
2	$\frac{1}{2}(*2a)$	$\frac{1}{2}(*10b)$	7.565

amplitude is inaccurate. (There is recent work on uniform approximations to account for such effects [33], unfortunately it seems not to apply to the cardioid, which has the additional curious feature that the boundary curvature is infinite at the vertex.)

We now consider some specific examples. The first two discrepancies occur at $L\approx6.6$ (o) and $L\approx7$ (*). In this region, the single-particle trace formula is erroneous [30] and these errors propagate through to the cross term and inevitably to the quantum-mechanical transform. We have also computed the cross term using quantum mechanics, i.e., using $\tilde{\rho}_1=\rho_1-\overline{\rho_1}$ in Eq. (45) and confirmed that these discrepancies do not arise (cf. Figs. 8 and 9). Thus, these discrepancies are due to errors in the semiclassical approximation of the cross term.

For the rest of the discussion, Λ refers to a particular periodic orbit family in the full phase space with each two-particle orbit in this family comprised of the single-particle orbits Γ_1 and Γ_2 and L_Λ are the lengths of the orbits in each family. Next, consider the peak structure at $L\approx7.5$ (+). There are two families of orbits, Λ_1 and Λ_2 that are responsible for these peaks. The underlying structures of these orbits are shown in Table I. Bearing in mind the two single-particle orbits Γ_2 are not well isolated (cf. Fig. 6), the Gutzwiller amplitude of each Γ_2 is incorrect. Consequently, the two-particle Gutzwiller amplitude will also be incorrect, as Fig. 7 demonstrates. Let us look at the next peak structure. Clearly, the quantum peak heights are underestimated at $L\approx8.1$ (X). We account for this by recognizing the two-particle orbit structure involves the single-particle orbit $\frac{1}{2}(*8b)$ that is an orbit which passes close to the vertex. More specifically, the orbit family $\Lambda=3$ is composed of single-particle orbits $\Gamma_1=\frac{1}{2}(*4b)$ and $\Gamma_2=\frac{1}{2}(*8b)$ and the lengths of these two-particle orbits are $L_\Lambda=8.109$. As a final illustration, we consider the region $9.6<L<10.3$. In this neighborhood, the semiclassics are particularly bad. This can be accounted for by inspection of Table II.

TABLE II. A few of the periodic orbits which conspire to give trouble around $L=10$.

Λ	Γ_1	Γ_2	L_Λ
4	$3a$	$4a$	9.684
5	$3a$	$\frac{1}{2}(*10b)$	9.687
6	$4a$	$\frac{1}{2}(*8b)$	9.740
7	$\frac{1}{2}(*8b)$	$\frac{1}{2}(*10b)$	9.742
8	$4a$	$4a$	10.044
9	$4a$	$\frac{1}{2}(*10b)$	10.046
10	$\frac{1}{2}(*10b)$	$\frac{1}{2}(*10b)$	10.048

As Table II and Fig. 6 show, there are many instances where both of the single-particle orbits constituting the full orbit are poorly isolated. In view of this, both single-particle Gutzwiller amplitudes are incorrect making the product even worse. This accounts for the gross inconsistencies in this region of the reciprocal space. The other discrepancies can be accounted for in a similar manner.

B. Symmetry decomposition

In this section, we explore the symmetry decomposition of the two-particle problem. We start by defining the smooth and oscillating symmetry reduced densities from Eq. (21)

$$\overline{\rho}_{S/A}(k)=\frac{1}{2}\left[(\overline{\rho}_1*\overline{\rho}_1)(k)\pm\frac{1}{\sqrt{2}}\overline{\rho}_1\left(\frac{k}{\sqrt{2}}\right)\right] \tag{48}$$

and

$$\tilde{\rho}^{\rm dyn}_{S/A}(k)=\frac{1}{2}\left[(\tilde{\rho}_1*\tilde{\rho}_1)(k)\pm\frac{1}{\sqrt{2}}\tilde{\rho}_1\left(\frac{k}{\sqrt{2}}\right)\right]. \tag{49}$$

While the second term in Eq. (49) is a single-particle density, in a future paper [20] we will demonstrate that this term arises from the physical situation in which two particles are traversing the same periodic orbit, with the same energy and are exactly half a period out of phase. It describes the effect of particle exchange on the spectrum and for this reason affects the symmetric and antisymmetric spaces differently and is based on the theory of Ref. [34]. Therefore, this second term also belongs to the two-particle dynamical term and we identify Eq. (49) as being a purely dynamical term. We want to compare it with the corresponding term in the symmetrized quantum density-of-states. Hence, in analogy with the previous subsection, we compare

$$\tilde{F}^{\rm dyn}_{S/A}(L)=\mathcal{F}\{\tilde{\rho}^{\rm dyn}_{S/A}(k)\} \tag{50}$$

and

$$\tilde{F}^{\rm qm}_{S/A}(L)=\mathcal{F}\{\rho_{S/A}(k)-\overline{\rho}_{S/A}(k)-\overline{\rho}_1*\tilde{\rho}_1(k)\}, \tag{51}$$

where $\rho_{S/A}(k)$ is the quantum bosonic (S) or fermionic (A) density-of-states.

C. Numerics for the symmetrized cardioid

In this section, we numerically compare the symmetrized quantum mechanics with the corresponding semiclassical quantities. In particular, we compute the transforms Eqs. (50) and (51) [35]. The symmetrized quantum densities are

$$\rho_S(k)=\sum_{i<j}\delta(k-\sqrt{k_i^2+k_j^2})+\sum_i\delta(k-\sqrt{2}k_i),$$
$$\rho_A(k)=\sum_{i>j}\delta(k-\sqrt{k_i^2+k_j^2}) \tag{52}$$

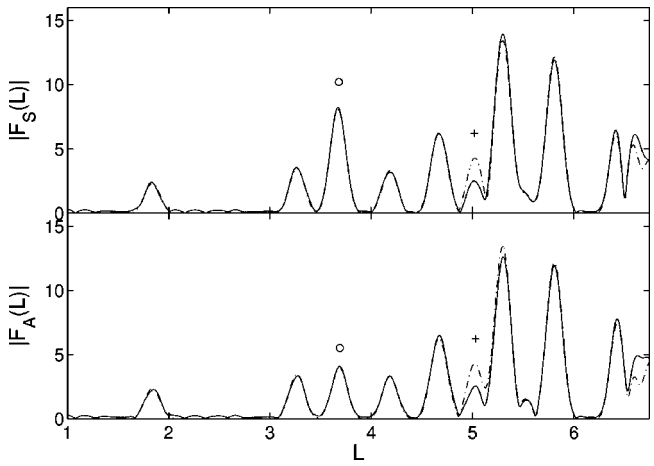

FIG. 10. The Fourier transform of the quantum and semiclassical symmetrized densities of states; the top is bosonic and the bottom is fermionic. In both cases the solid line is the transform of the quantum density-of-states and the dashed-dotted line is the transform of its semiclassical approximation. Peaks with symbols are described in the text.

using the same constraint on the energies as above. Of course, the sum of these symmetrized densities is the total density-of-states.

Before presenting our numerical results, we describe what we expect. First, all the peaks of the unsymmetrized two-particle density should be present. In addition, for each single-particle periodic orbit Γ, there should also be peaks at lengths $L_\Gamma/\sqrt{2}$ arising from the oscillating part of the single-particle density-of-states. The results are shown in Fig. 10. For the two-particle density term of Eq. (50), we used the same 100 two-particle orbits of Sec. VI A while in the single density term we used all single-particle orbits with length $L<11$. As well, we included the single-particle orbit $\frac{1}{2}(*10h)$ (not shown in Fig. 6) which has a length $L=10.477$. Figure 10 displays the peak structure in the reciprocal space up to $L=6.75$.

We notice that most of the amplitude divides evenly between the symmetric and the antisymmetric densities. Nonetheless, there are exceptions such as the peak at $L\approx 3.6$ (o). Here, both terms of Eq. (49) contribute and the difference in the sign of the second term accounts for the uneven amplitude division between the two symmetrized densities. Semiclassically, we account for this peak structure by noting that two different physical situations are responsible for producing it. First, there is the situation in which both particles are on the orbit $\Gamma=\frac{1}{2}(*2a)$ with no restrictions on the time phase difference between the two particles. This contribution comes from the two-particle density term resulting in a peak at a length $\sqrt{2}L_\Gamma=3.673$ and produces identical structures in both densities. The second situation occurs when both particles are on the orbit $\Gamma=(*2a)$ exactly half a period out of phase. This contribution comes from the single density term at $L_\Gamma/\sqrt{2}=3.673$ and is explained more fully in Ref. [20]. Since the second contribution comes with a different sign in the two symmetries, the amplitudes are different for the symmetric and antisymmetric spaces. In this particular case, it is

stronger in the symmetric density and weaker in the antisymmetric density, although the opposite may be true in other cases.

In closing, we remark that the overall agreement between the quantum and semiclassical calculations is good. The poorly reproduced peak just above $L=5$ (+) comes from the single density term. This is just the poorly reproduced peak of the single-particle density at $L\approx 7$ shifted down by a factor of $\sqrt{2}$.

VII. CONCLUSION

In this paper, we have presented a semiclassical formalism for the two-particle density of states. After deriving a trace formula that explicitly involves two-particle dynamics, we investigated its structure and noted intuitive properties such as the additivity of the actions and topological phase factors. As well, we briefly explained the structure of the full two-particle orbits, which come in degenerate families. Then, we considered two-particle billiards, obtaining approximate formulas for all terms in the semiclassical density-of-states, including a detailed discussion of spurious end point contributions.

Following these general considerations, we studied two identical noninteracting particles in a disk and in a cardioid. In each case, we find that the formalism correctly reproduces the full and symmetrized densities-of-states. The semiclassical symmetry decomposition involved formal substitution of the semiclassical quantities into the quantum-mechanical expressions for the symmetrized densities. In future work [20], we will show how these formal expressions emerge directly from the classical structures. In the integrable problem, we found that our formalism replicates the two-body EBK spectrum more precisely than the quantum spectrum, suggesting a deep connection between periodic orbit theory and EBK quantization for integrable systems. In the chaotic cardioid billiard, we note that the single-particle orbits that pass close to the vertex lead to inconsistencies in the Fourier transform of the semiclassical density-of-states. Clearly, our formalism fails here because the Gutzwiller theory itself fails for these ''semidiffractive'' orbits. For all other orbits, the two-particle trace formula works very well.

The techniques employed here involve the classical phase space of each particle. In a future paper [20], we derive the same results by working in the full two-particle phase space. This approach has the advantage of being more general than what we have presented here. Nonetheless, it is conceptually useful to see how the same structure emerges from these two distinct points of view. We would also like to incorporate interactions between the particles. Such a project would undoubtedly require working in the full phase space since it is no longer true that the full density-of-states is the convolution of the single-particle level densities. This provides an additional motivation for working out the noninteracting problem in the full phase space as a first step towards the more ambitious goal. This full phase space analysis also generalizes more readily to more particles. Finally, it has the conceptual advantage that the spurious end-point contributions discussed in Sec. IV D and Appendix B do not arise and therefore need not be explained away.

It may be argued that interacting many-body systems are too complex to be accessible to the semiclassical method. However, given the intractability of the many-body problem, there may be questions which semiclassical theory can answer. In particular, we have in mind the applications of semiclassical theory to mesoscopic physics [19]. Here, our seemingly academic study of billiard systems finds physical applications in the context of nanostructures. For example, the disk billiard can serve as a realistic lowest-order approximation to the mean field of the electrons in a circular quantum dot [36]. In fact, many phenomena in ballistic mesoscopic systems can, at least qualitatively, be described by using quantum billiards with independent particles as physical models.

ACKNOWLEDGMENTS

The authors are grateful to the NSERC for financial support. We thank Rajat Bhaduri, Matthias Brack, and Randy Dumont for useful discussions.

APPENDIX A: NONIDENTICAL PARTICLES

As we have mentioned, most of the discussion still applies if the two particles are not identical. The main differences are that one no longer considers the symmetrized density-of-states since the symmetry of particle exchange no longer exists and secondly there are two distinct cross terms so that Eq. (11) is replaced by

$$\rho_2(E)=\overline{\rho}_{1a}*\overline{\rho}_{1b}(E)+\overline{\rho}_{1a}*\widetilde{\rho}_{1b}(E)+\widetilde{\rho}_{1a}*\overline{\rho}_{1b}(E)+\widetilde{\rho}_{1a}*\widetilde{\rho}_{1b}(E), \tag{A1}$$

where the indices a and b refer to the two distinct particles, while the indices 1 and 2 still refer to one- or two-particle densities-of-states.

Suppose, for example, that we have two nonidentical particles in a billiard. We introduce two parameters, $\alpha_a=2m_a/\hbar^2$ and $\alpha_b=2m_b/\hbar^2$. The smooth term (23) is replaced by

$$\overline{\rho}_{1a}*\overline{\rho}_{1b}(E)\approx\frac{\alpha_a\alpha_b\mathcal{A}^2}{16\pi^2}E-(\sqrt{\alpha_a}+\sqrt{\alpha_b})\frac{\sqrt{\alpha_a\alpha_b}}{16\pi^2}\mathcal{A}\mathcal{L}\sqrt{E}+\frac{\sqrt{\alpha_a}\sqrt{\alpha_b}\mathcal{L}^2}{64\pi}+\frac{(\alpha_a+\alpha_b)\mathcal{A}\mathcal{K}}{4\pi}. \tag{A2}$$

The cross terms each separately have the same structure as the cross term for identical particles. Obviously, they are no longer equal to each other, but functionally little has changed. It is just a matter of inserting the relevant information from the different smooth and oscillating densities-of-states of the two particles. Following the same logic as before, we find

$$I_{\mathcal{A}}(E)\approx\frac{\alpha_a\mathcal{A}}{4\pi^2}\sum_{\Gamma_b}\frac{A_{\Gamma b}}{T_{\Gamma b}}\cos\left(\Phi_{\Gamma_b}-\frac{\pi}{2}\right), \tag{A3}$$

$$I_{\mathcal{L}}(E)\approx-\frac{\sqrt{\alpha_a}\mathcal{L}}{8\pi^{3/2}\sqrt{\hbar}}\sum_{\Gamma_b}\frac{A_{\Gamma b}}{\sqrt{T_{\Gamma b}}}\cos\left(\Phi_{\Gamma_b}-\frac{\pi}{4}\right),$$

$$I_{\mathcal{K}}(E)\approx\frac{\mathcal{K}}{\pi\hbar}\sum_{\Gamma_b}A_{\Gamma b}\cos(\Phi_{\Gamma_b}),$$

where $\Phi_{\Gamma_b}=\sqrt{\alpha_b E}L_{\Gamma_b}-\sigma_{\Gamma_b}\pi/2$. For $\overline{\rho}^{*}_{1b}\widetilde{\rho}_{1a}(E)$, we just interchange a and b.

The formula for $\widetilde{\rho}_{1a}*\widetilde{\rho}_{1b}(E)$ still has the same basic structure, but should obviously use distinct periodic orbits for particles a and b. In particular, Eqs. (12) and (18) still apply, but with two important differences. First, the double sums over periodic orbits are now labeled by the distinct periodic orbits of the two particles. Second, the energy partition will change due to differing masses. The criterion of stationary phase will still specify that the two particles have the same period, but relations such as Eqs. (28) and (29) do not apply since they assume equal masses. The generalizations are rather straightforward to determine. For example, the saddle energies (29) are replaced by

$$\frac{E_0}{E}=\frac{m_aL_{\Gamma_a}^2}{m_aL_{\Gamma_a}^2+m_bL_{\Gamma_b}^2},\quad\frac{E-E_0}{E}=\frac{m_bL_{\Gamma_b}^2}{m_aL_{\Gamma_a}^2+m_bL_{\Gamma_b}^2},\tag{A4}$$

while the general dynamical expression for billiards (31) is replaced by

$$\begin{aligned}\widetilde{\rho}_{1a}*\widetilde{\rho}_{1b}(E)\approx&\frac{(2E)^{3/4}\sqrt{\alpha_a\alpha_b\hbar}}{(2\pi)^{3/2}}\\&\times\sum_{\Gamma_a,\Gamma_b}\frac{L_{\Gamma_a}L_{\Gamma_b}}{(m_aL_{\Gamma_a}^2+m_bL_{\Gamma_b}^2)^{5/4}}A_{\Gamma_a}\\&\times(E_0)A_{\Gamma_b}(E-E_0)\\&\times\cos\left[\sqrt{\alpha_aL_{\Gamma_a}^2+\alpha_bL_{\Gamma_b}^2}\sqrt{E}\right.\\&\left.-(\sigma_{\Gamma_a}+\sigma_{\Gamma_b})\frac{\pi}{2}-\frac{\pi}{4}\right].\end{aligned}\tag{A5}$$

In the special case of identical particles, it is simple to check that this expression reduces to Eq. (31). For lack of an immediate physical context, we do not explore this case any further.

Another situation is a single particle in a separable potential. For example, in two dimensions, one could have $V(x,y)=V_a(x)+V_b(y)$ in which case, the dynamics in the x direction are completely uncoupled from the dynamics in the y direction so that the system is formally the same as if there were distinct particles executing the x and y motions.

APPENDIX B: SPURIOUS END-POINT CONTRIBUTIONS FOR ISOLATED BILLIARD ORBITS

Here we evaluate the cross term integrals exactly for isolated periodic orbits. This allows us to do an asymptotic expansion to explicitly demonstrate that the additional end-point contributions not included are spurious. We must evaluate the integral

$$\overline{\rho_1}*\widetilde{\rho}_1(E)=\int_0^E d\epsilon\,\overline{\rho_1}(\epsilon)\widetilde{\rho}_1(E-\epsilon),\tag{B1}$$

where $\overline{\rho_1}(\epsilon)$ is given by the Weyl expansion (3) and $\widetilde{\rho}_1(\epsilon)$ for a billiard with isolated orbits is given by

$$\widetilde{\rho}_1(\epsilon)\approx\frac{\sqrt{\alpha}}{2\pi\sqrt{\epsilon}}\sum_{\Gamma}\frac{L_\gamma}{\sqrt{|\det(\widetilde{M}_\Gamma-I)|}}\cos\left(\sqrt{\alpha\epsilon}L_\Gamma-\sigma_\Gamma\frac{\pi}{2}\right).\tag{B2}$$

This gives

$$\begin{aligned}\overline{\rho_1}*\widetilde{\rho}_1(E)\approx\sum_{\Gamma}\frac{L_\gamma}{\sqrt{|\det(\widetilde{M}_\Gamma-I)|}}&\left(\alpha^{3/2}\frac{\mathcal{A}}{8\pi^2}I_1\right.\\&\left.-\alpha\frac{\mathcal{L}}{16\pi^2}I_2+\alpha^{1/2}\frac{\mathcal{K}}{2\pi}I_3\right),\end{aligned}\tag{B3}$$

where

$$\begin{aligned}I_1&=\int_0^E d\epsilon\frac{1}{\sqrt{E-\epsilon}}\cos\left(\sqrt{\alpha(E-\epsilon)}L_\Gamma-\sigma_\Gamma\frac{\pi}{2}\right),\\I_2&=\int_0^E d\epsilon\frac{1}{\sqrt{\epsilon}}\frac{1}{\sqrt{E-\epsilon}}\cos\left(\sqrt{\alpha(E-\epsilon)}L_\Gamma-\sigma_\Gamma\frac{\pi}{2}\right),\\I_3&=\frac{1}{\sqrt{E}}\cos\left(\sqrt{\alpha E}L_\Gamma-\sigma_\Gamma\frac{\pi}{2}\right).\end{aligned}\tag{B4}$$

If we evaluate the first two integrals exactly, we get

$$I_1=\frac{2}{\sqrt{\alpha}L_\Gamma}\left[\cos\left(\Phi_\Gamma+\phi_\Gamma-\frac{\pi}{2}\right)-\cos\left(\phi_\Gamma-\frac{\pi}{2}\right)\right]\tag{B5}$$

and

$$\begin{aligned}I_2&=\pi\cos\phi_\Gamma J_0(\Phi_\Gamma)-\pi\sin\phi_\Gamma\mathbf{H}_0(\Phi_\Gamma)\\&\approx\sqrt{\frac{2\pi}{\sqrt{\alpha E}L_\Gamma}}\cos\left(\Phi_\Gamma+\phi_\Gamma-\frac{\pi}{4}\right)-\frac{2}{\sqrt{\alpha E}L_\Gamma}\cos(\phi_\Gamma)+\cdots,\end{aligned}\tag{B6}$$

where $\Phi_\Gamma=\sqrt{\alpha E}L_\Gamma$, $\phi_\Gamma=-\sigma_\Gamma\pi/2$, J_0 is a zero-order

Bessel function, and $\mathbf{H}_0$ is a zero-order Struve function. In the second line of Eq. (B6), we have used the asymptotic expansions of these two functions.

In both I_1 and I_2, we note that asymptotically there are terms with two distinct structures. The first are terms that are sinusoidal in $\sqrt{E}$ and correspond exactly to what was used in the cross term for the cardioid [i.e., Eqs. (25) and (26)]. There are also terms which are nonsinusoidal in E. In I_1, this comes directly from the upper end point of the integral while in I_2 it comes from the expansion of the Struve function. In each term, the nonsinusoidal terms arise from the end point around $\epsilon = E$ which, as we argued in Sec. IV D, corresponds to an unphysical situation. Therefore, keeping only the asymptotically appropriate term (i.e., the oscillatory one) yields the correct behavior for the cross term.

A similar analysis would yield similar results for the spurious end-point contributions in the cross term of the disk billiard and the dynamical term of either billiard.

[1] M. C. Gutzwiller, J. Math. Phys. **8**, 1979 (1967); **10**, 1004 (1969); **11**, 1791 (1970); **12**, 343 (1971); *Chaos in Classical and Quantum Mechanics* (Springer-Verlag, New York, 1990).

[2] R. Balian and C. Bloch, Ann. Phys. (N.Y.) **60**, 401 (1970); **63**, 592 (1971); **69**, 76 (1972); **85**, 514 (1974).

[3] M. V. Berry and M. Tabor, Proc. R. Soc. London, Ser. A **349**, 101 (1976); J. Phys. A **10**, 371 (1977).

[4] P. Cvitanović *et al.*, *Classical and Quantum Chaos: A Cyclist Treatise* (Niels Bohr Institute, Copenhagen, 2000) (http://www.nbi.dk/ChaosBook/).

[5] M. Brack and R. K. Bhaduri, *Semiclassical Physics* (Addison-Wesley, Reading, MA, 1997).

[6] P. Cartier and A. Voros, C. R. Acad. Sci. (Paris) Sér. I **307**, 143 (1988); A. Voros, Suppl. Prog. Theor. Phys. **116**, 17 (1994).

[7] M. V. Berry and C. J. Howls, Proc. R. Soc. London, Ser. A **447**, 527 (1994).

[8] H. M. Sommermann and H. A. Weidenmüller, Europhys. Lett. **23**, 79 (1993).

[9] H. A. Weidenmüller, Phys. Rev. A **48**, 1819 (1993).

[10] T. Papenbrock and T. H. Seligman, Phys. Lett. A **218**, 229 (1996).

[11] T. Papenbrock, T. H. Seligman, and H. A. Weidenmüller, Phys. Rev. Lett. **80**, 3057 (1998); T. Papenbrock and T. Prozen, *ibid.* **84**, 26 (2000).

[12] S. W. McDonald, Ph.D. thesis, Lawrence Berkeley Laboratory, Report No. LBL-14837, 1983; E. J. Heller, Phys. Rev. Lett. **53**, 1515 (1984); E. B. Bogomolny, Physica D **31**, 169 (1988); M. V. Berry, Proc. R. Soc. London, Ser. A **423**, 219 (1989).

[13] L. Benet *et al.*, e-print chao-dyn/9912035.

[14] K. Richter, G. Tanner, and D. Wintgen, Phys. Rev. A **48**, 4182 (1993); G. S. Ezra *et al.*, J. Phys. B **24**, L413 (1991); D. Wintgen, K. Richter, and G. Tanner, Chaos **2**, 19 (1992).

[15] K. Richter, *Semiclassical Theory of Mesoscopic Quantum Systems* (Habilitationsschrift, Augsburg, 1997).

[16] D. Ullmo *et al.*, Physica E **1**, 268 (1997).

[17] D. Ullmo *et al.*, Phys. Rev. Lett. **80**, 895 (1998).

[18] K. Tanaka, Ann. Phys. (N.Y.) **268**, 31 (1998).

[19] K. Richter, D. Ullmo, and R. Jalabert, Phys. Rep. **276**, 1 (1996); R. Jalabert, e-print cond-mat/9912038.

[20] J. Sakhr and N. D. Whelan (unpublished).

[21] K. Stewartson and R. T. Waechter, Proc. Cambridge Philos. Soc. **69**, 353 (1971).

[22] R. K. Bhaduri *et al.*, Phys. Rev. A **59**, R911 (1999).

[23] H. R. Krishnamurthy, H. S. Mani, and H. C. Verma, J. Phys. A **15**, 2131 (1982).

[24] V. M. Strutinsky, Nukleonika **20**, 679 (1975); V. M. Strutinsky and A. G. Magner, Fiz. Elem. Chastits At. Yadra **7**, 356 (1976) [Sov. J. Part. Nucl. **7**, 138 (1976)]; S. C. Creagh and R. G. Littlejohn, Phys. Rev. A **44**, 836 (1991); J. Phys. A **25**, 1643 (1992).

[25] J. Sakhr, Master's thesis, McMaster University, 1999 (unpublished).

[26] S. M. Reimann *et al.*, Phys. Rev. A **53**, 39 (1996).

[27] For a separate example, imagine a single particle in a three-dimensional stadium billiard constructed by rotating the two-dimensional stadium around its long axis. The dynamics is still largely chaotic although there is a constant of motion, the azimuthal angular momentum. This will be reflected in the quantum spectrum where all states will be eigenstates of the angular momentum operator. If we analyze all of the states together, we observe a Poisson spacing distribution even though separately each spectrum is closer to having a Wigner-like spacing distribution.

[28] R. Markarian, Nonlinearity **6**, 819 (1993).

[29] G. Vattay, A. Wirzba, and P. E. Rosenqvist, Phys. Rev. Lett. **73**, 2304 (1994); N. D. Whelan, Phys. Rev. E **51**, 3778 (1995); N. Pavloff and C. Schmit, Phys. Rev. Lett. **75**, 61 (1995); N. D. Whelan, *ibid.* **76**, 2605 (1996).

[30] H. Bruus and N. D. Whelan, Nonlinearity **9**, 1023 (1996).

[31] A. Bäcker, F. Steiner, and P. Stifter, Phys. Rev. E **52**, 2463 (1995); A. Bäcker and H. R. Dullin, J. Phys. A **30**, 1991 (1997).

[32] F. J. Harris, Proc. IEEE **66**, 51 (1978).

[33] M. Sieber, N. Pavloff, and C. Schmit, Phys. Rev. E **55**, 2279 (1997).

[34] J. M. Robbins, Phys. Rev. A **40**, 2128 (1989).

[35] We use different window function parameters for the single and two-particle densities in Eqs. (50) and (51), although this is not strictly necessary. For single-particle densities, the parameters k_0 and k_f are chosen so the window function goes smoothly to zero at the end points of the single-particle spectrum. For two-particle densities, we use the same window function as before.

[36] M. Persson *et al.*, Phys. Rev. B **52**, 8921 (1995).